

On the effect of subinertial phenomena on the internal lee waves generation in the Strait of Gibraltar

José J. del Alonso Rosario · M. Arias Ballesteros ·
P. Villares Durán

Published online: 18 July 2006
© Springer-Verlag 2006

Abstract The generation of internal lee waves (ILW) in the Strait of Gibraltar takes place in the main sill where the tidal flow interacts with a submarine obstacle. The tidal flow is perturbed by subinertial phenomena of different nature summarized in the subinertial currents that can inhibit the ILW generation. The authors present an attempt to randomize the problem by the introduction of a Gaussian noise in the Taylor–Goldstein equation. The random number sets are generated from the statistical distribution of the previously isolated random part of the subinertial currents from experimental data taken in the area during the Gibraltar Experiment 94–96. The effect of the noise is translated into a continuous spreading of the spectrum around the solution of the noise-free problem. A stability analysis is carried out in order to determine the single neutral modes of oscillations and the phase space is divided onto regions of stability and instability as a function of the inflowing subinertial current. The methodology and results could be useful for the design and timing of oceanographic surveys in straits where the ILWs occur.

Keywords Subinertial currents · Internal lee waves · Camarinal sill

1 Introduction

The Strait of Gibraltar is the natural channel between the Atlantic and the Mediterranean. Lacombe and Richez (1982, 1984) identified three scales of motion in the strait: long period (longer than annual), related to the two-layer water masses exchange; subinertial (with periods greater than the inertial period of the location), related to the meteorological; and tidal forcing. All of them consider the water masses exchange between the Atlantic and the Mediterranean basins. Alonso and Andonegui (2005) added a fourth scale of shorter period, from minutes to 3 or 4 h, associated with internal waves. This is responsible for the vertical mixing between the Atlantic and Mediterranean layers if a two-layer model of the Strait of Gibraltar is assumed and the internal waves, hydraulic jump and lee waves fall in this new category. The observations reported in the CANIGO project (CANIGO 1999), Bruno et al. (2002), Echevarría et al. (2002) and the prediction model developed in Alonso et al. (2003) are the basis for the addition of the fourth time scale (Alonso and Andonegui 2005).

The internal waves at the Strait of Gibraltar are well known oceanographic phenomenon. The classical internal bore is present when critical conditions occur over Camarinal sill. There are many references to this phenomenon in the literature but they are focused on the generation, propagation and release towards the Mediterranean of internal waves (Frassetto 1964; Ziegenbein 1969; Cavanie 1972; La Violette et al. 1986; La Violette and Lacombe 1988; Richez 1994; Bray et al. 1990; Watson and Robinson 1990; Bray et al. 1990; Brandt et al. 1996; Morozov et al. 2002, among many others). Bruno et al. (2002) reported a new type

J. J. del Alonso Rosario (✉) · M. Arias Ballesteros ·
P. Villares Durán
Applied Physics Department, Physical Oceanography,
University of Cádiz, Polígono del Río San Pedro s/n,
Puerto Real, 11510 Cádiz, Spain
e-mail: josejuan.alonso@uca.es

of internal wave, classified after as internal lee wave (ILW) by Alonso et al. (2003). A discussion of the role of these waves in the mixing process in the Strait of Gibraltar was given in Echevarría et al. (2002). A full discussion and an analytical high order model were presented in Alonso and Andonegui (2005). This happens in subcritical conditions when a suitable combination of the stratification and the incoming flow allows the upward propagation of hydrodynamic perturbations generated at the bottom. In Alonso et al. (2003) a study of the conditions for the generation, vertical propagation and a linear prediction model for ILW generation were developed. In addition the *topographic criterion of existence* and a *critical velocity* were also established and it was demonstrated that the water mass exchange is not always maximal through the Strait of Gibraltar. In the opinion of the authors, the first and only very basic attempt to describe the effect of the subinertial currents on the generation of ILW can be found in the same publication. One of its main conclusions is that subinertial currents can distort and inhibit the generation of ILW.

On the other hand, the driving force of the subinertial fluxes has been related to the air pressure fluctuations over the Mediterranean basin (Crepon 1965; Garrett et al. 1989; Candela et al. 1989, 1990). Subinertial and tidal flows have a similar distribution with the maximum values at Camarinal sill decreasing to the east and west of the sill (Pillsbury et al. 1987). They can be considered as barotropic and responsible for 93.4 and 84% motion of the semidiurnal and the subinertial frequency band, respectively (Candela et al. 1990). Garrett (1989) showed the relationship between the non-astronomical signal of M2 in the water column and the fluctuations of subinertial currents along the Strait. Tsimplis (2000) and Bruno et al. (2002) explained the vertical structure of currents in the Strait of Gibraltar and Mañanes et al. (1998) showed that the distortions of the barotropic M2 wave are correlated with the barotropic mode of the subinertial currents. These lead to the idea that the subinertial currents in the Strait of Gibraltar have an important baroclinic component. Their measurements carried out at one point showed that they introduce large deviations in amplitude and phase lags.

The same kind of ILW has been found in the Kuril Straits and they have been reported in Nakamura et al. (2000). They showed that the phenomenon does not follow the classical theories of internal waves, including the concept of *critical slope* (Wunsch 1969; Baines 1982; Huthnance 1989), and the inability of the modal decomposition to explain and characterise the short period internal waves. In addition, Nakamura and

Awaji (2001) show that the actual models as those studied by Hibiya (1986) and Gerkema and Zimmerman (1995) cannot explain the observed ILW. In Nakamura and Awaji (2001) they find the solution using the method of characteristics applying the same model that Nakamura et al. (2000) and assume the hypothesis that the growth of the ILW is due to advection. This conclusion was also demonstrated by Lott and Teitelbaum (1993a, b) for the amplification of unsteady atmospheric lee waves. In Nakamura et al. (2000) and Nakamura and Awaji (2001) a single tidal wave is considered in the simulations and the vertical profile of velocities is not perturbed by subinertial currents as in the Strait of Gibraltar. In Nakamura et al. (2000) and Nakamura and Awaji (2001) a single tidal wave is considered in the simulations and the vertical profile of velocities is not perturbed by subinertial currents as in the Strait of Gibraltar. However their results coincide with Bruno et al. (2002), Echeverría et al. (2002) and Alonso et al. (2003) about a very important role of the ILW in mixing the water masses. The hydrodynamic conditions are subcritical at the top of the sill.

In addition, there is an unavoidable and additional complexity not contemplated in Nakamura et al. (2000) and Nakamura and Awaji (2001). This is related to the physics of resonant processes and the possibility of Holmboe's waves. This kind of waves occurs when the dimensions of the physical system verify that the flow becomes stable for all generated wavelengths (Hazel 1972), hence all internal waves (even the short period ones) can be generated and all of them become resonant. The Holmboe's critical limit depends on the potential function of the associated Sturm–Liouville problem as shown in Hazel (1972). This hypothesis must be considered since the Taylor–Goldstein equation can be obtained from the mathematical model of Nakamura et al. (2000).

The two objectives of this work are (1) the study and characterization of the subinertial currents at the Strait of Gibraltar and (2) the inclusion and the analysis of the effect of the subinertial currents on the wavelength of the ILW generated in subcritical conditions at the main sill of the Strait of Gibraltar.

The outline of this work is as follows. In Sect. 2, the description of the data and the area under study is given. Section 3 is devoted to make review of the subinertial currents in the Strait of Gibraltar. Section 4 is devoted to establish the conceptual framework. In the Sect. 5 the statistical vertical structure of the subinertial currents at the main sill of the Strait of Gibraltar and the characterisation of the Gaussian noise are developed. In Sect. 6, the numerical experiments are

commented upon and described. Section 7 is devoted to obtaining of the dispersion relationships and stability of the analysed conditions. Finally, the conclusions are outlined in Sect. 8.

2 Data description and pre-processing

Data used in this study are the same of those fully described in previous works by Bruno et al. (2002), Echevarría et al. (2002), Alonso et al. (2003) and Alonso and Andonegui (2005). They consist of two types of data. The first set is the data from an ADCP taken in the Gibraltar 94/96 experiment. Two years of hourly data current from an upward looking 150 kHz ADCP moored at the top of Camarinal sill in the Strait of Gibraltar (Fig. 1) have been used. The mooring was located in the generation area of the internal waves in the Strait of Gibraltar where the highest velocities are observed. Small gaps of less than one day were due to the operations of recovering, data reading, cleaning and repeated deploying of the ADCP. Periods of mooring are detailed in Table 1. Available depths are from 45 to 245 m with a 10 m interval and the data close to the surface and bottom were not considered

because of the reflections of acoustic beams. The subinertial currents have been obtained by filtering with a low-pass filter with a cut-off frequency of 1 cycle/day. The newly formed velocity time series were re-sampled to one value per day and named u_{depth}^2 . Although some CTD measurements were taken in the same survey [see Bruno et al. (2002) and Echevarría et al. (2002) for full description] they are not useful for the prediction of the ILW because they are distorted by them.

The second set is CTD data from two surveys performed during CANIGO project on June 18–25, 1997 and September 2–9, 1997 (Echevarría et al. 2002; Bruno et al. 2002). The CTD profiles were taken with a Phalmouth multi-parameter probe with CTD, fluorimeter and nephelometer. Profiles were repeated hourly during a semidiurnal tidal cycle. The resulting profile used in this study is the average of the CTD profiles taken close to the sill in the Strait of Gibraltar and it was parameterized to a five parameters sigmoidal function [see Alonso and Andonegui (2005) for full details] to make easier the handle in the theoretical models:

$$\rho(z) = \rho_0 + \frac{\rho_a}{\left(1 + \exp\left(-\frac{z - \rho_{z_0}}{\rho_b}\right)\right)^{\rho_c}}. \quad (1)$$

Fig. 1 The Strait of Gibraltar. The ADCP was moored at the Camarinal sill, marked with *D*, in the Gibraltar Experiment 94/96

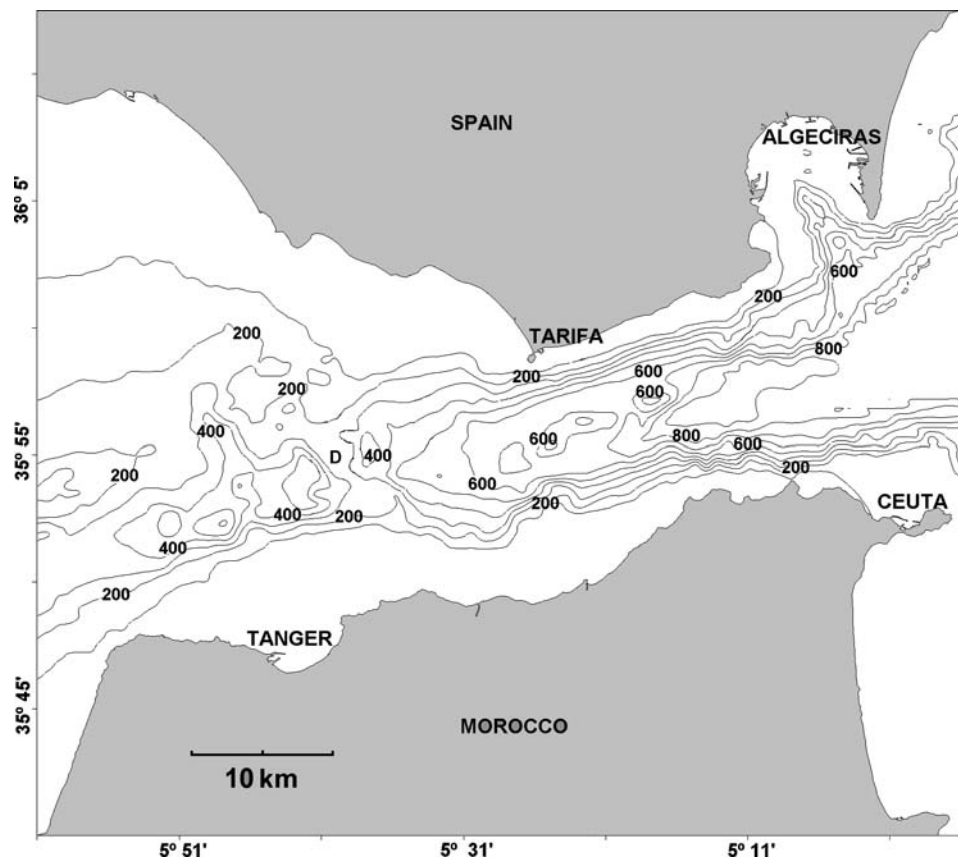


Table 1 Start time and number of data available for each moored period

Start time	Number of data
15 00 hours 21-10-1994	3,954
18 45 hours 06-04-1995	4,554
13 15 hours 16-10-1995	4,494
11 15 hours 21-04-1996	3,739

The coefficients were computed by non-linear least squares following the Levenberg–Marquardt method (Press et al. 1986). The resulting values are $\rho_a = 3.36$; $\rho_b = -10.08$, $\rho_c = 1.29$ and $\rho_0 = 26.5$. (Alonso et al. 2003; Alonso and Andonegui 2005). The depth of the interface is computed from the vertical profiles of velocity following Tsimplis and Bryden (2000). They found a maximum difference between the depth of the interface from CTD data and the inflexion point from the vertical profile of velocity of 8 m. Hence, the depth of the interface can be deduced from the vertical profile of velocities and this is computed from the harmonic prediction of currents.

Because the CTD and ADCP data sets are not simultaneous some errors are introduced in the computation, but the parameterization is quite good as shown in Bruno et al. (2002), Alonso et al. (2003) and Alonso and Andonegui (2005).

3 Subinertial currents in the Strait of Gibraltar

Many efforts have been made and reported in the literature about the subinertial currents in the Strait of Gibraltar. It is possible to consider that the subinertial currents in the Strait of Gibraltar have several sources. The main and most obvious is the tidal forcing. The tidal flow interacts with the bottom topography producing baroclinic contributions to the currents in all tidal bands. Mañanes et al. (1998) studied the interaction of the M2 tidal wave with the subinertial barotropic flows; Tsimplis (2000) gave the structure of the vertical modes for waves on various time scales but for the vertical modes associated to the long tidal waves the results are not definite. The other considered source of perturbations is the fluctuating field of air pressure over the Mediterranean basin studied by Crepon (1965) and Garrett et al. (1989) among others.

Two of the most interesting subinertial tidal waves are the fortnightly, Msf, and the monthly, Mm, because they are used to present anomalous values. Experimental evidences for these components are available (Geyer and Cannon 1982; Griffin and LeBlond 1990; Freeland and Farmer 1980; de Silva Samaringhe and Lennon 1987; Nunes and Lennon 1987; Valle-Levinson

and Wilson 1994; Candela et al. 1989, 1990) and numerical models have been developed in order to explain such observations (Hibiya et al. 1998). Hence, the attention is focused on Mm and Msf and, in order to show why the subinertial currents in the Strait of Gibraltar cannot be predicted by classical methods such as harmonic analysis, in which the knowledge of only the harmonic constants of the two waves is considered. The amplitudes (in m/s) and phase lags (in degrees) for three selected depths are presented in Table 2. The values of the amplitudes of both waves are quite constant for the four phases of the experiment. However there are many variations in the phase lag with large variations up to 60° or more. The harmonic analysis will give an average value of the phase lag for the analyzed period that will be far from the perturbed instantaneous value. Hence as a hypothesis, it is possible to postulate that the main effect of the pressure fluctuation over the Mediterranean will result in at the Strait of Gibraltar as strong variations in the phase lag values of the subinertial waves. Then the harmonic prediction of the long tidal waves (subinertial) will not reproduce the behaviour of the tidal waves and another approach is needed to parameterize the long period band. In the absence of more information that allows the correct prediction of the phase lag of the subinertial waves, these deviations can be considered as noise.

4 Conceptual framework

The conceptual model has suffered some corrections before be definitively stated. The basic and partially

Table 2 Harmonic constants of Mm and Msf tidal waves for 75, 125 and 225 m depth for the four phases of the Gibraltar Experiment 94/96

Depth (m)	Mm (A, ϕ)	Msf (A, ϕ)
Phase 1		
75	0.0803, 170.32	0.1442, 221.74
125	0.0547, 169.56	0.1541, 226.61
225	0.1236, 14.08	0.2196, 28.57
Phase 2		
75	0.0921, 223.22	0.1997, 210.39
125	0.0907, 215.94	0.1980, 212.15
225	0.1122, 14.29	0.1968, 36.47
Phase 3		
75	0.0869, 144.05	0.1454, 205.44
125	0.0932, 139.45	0.1485, 210.60
225	0.1330, 25.05	0.2087, 29.11
Phase 4		
75	0.0746, 214.36	0.1356, 223.34
125	0.0806, 220.39	0.2055, 218.01
225	0.0947, 10.73	0.1753, 31.95

Amplitudes are expressed in m/s and phase lags in degrees

erroneous conceptual model was described in Bruno et al. (2002) and in Alonso et al. (2003) as heritage. The final conceptual frame was stated in Alonso and Andonegui (2005) and a brief outline is now given in order to fix concepts.

The generation of ILW is an internal resonant process that depends on the background velocity profile and on the stratification conditions (Hazel 1972; Bruno et al. 2002; Alonso et al. 2003; Alonso and Andonegui 2005). Because of this they can be also named internal resonant waves (IRW), meaning the same as ILW. The triggering mechanism is the interaction of the flow with the topography. The composite densimetric Froude number is always taken less than unit and the hydraulic jump has nothing to do. Close to the bottom a perturbation occurs due to the advection terms in the equations of motion. When the conditions for the upward propagation are favorable ($\omega = Uk < N$, ω is the frequency of the internal wave, U is the background velocity, k is the wave number and N is the root squared of the buoyancy frequency) an harmonic solution is obtained and it can propagate upward, otherwise the energy will be dissipated (damped solution) (Gill 1982; Konyaev and Sabinin 1992). Considering a zero relative velocity ($c = 0$), the internal wave is arrested by the flow (Bogucki et al. 1999). Following the results of Nakamura et al. (2000) and Nakamura and Awaji (2001), the energy reflection at the surface has no effect and it could be neglected. This is exact and introduces a difference with the previous and partially no-accurate conceptual model presented in Bruno et al. (2002) and in Alonso et al. (2003), as heritage, that stated it as a crucial point in the theory. This was properly modified in Alonso and Andonegui (2005). Then the conditions for resonance are observed and the internal wave will be non linear amplified, producing a very strong mixing (see Echevarría et al. 2002) with a constant energy input radiating from the bottom. The study of the vertical propagation angles for a three layer water column can be found in Alonso et al. (2003) following the Garrett and Munk (1972) scheme. Because the tidal forcing is the driving force of the process and it is time dependent, the ILW must be named unsteady lee waves (Nakamura et al. 2000) and they will occur as pulses (Alonso et al. 2003). With this, the ILW and the internal bore in the Strait of Gibraltar are excluding and alternating processes.

5 Determination of the subinertial noise

At the present, it is no possible to predict subinertial currents in the Strait of Gibraltar as it was pointed out.

Because these currents are important in the determination of ILW wavelengths (Alonso et al. 2003), a statistical approach is needed in order to obtain the probabilities of wavelengths occurrence. For the purposes of this study a Gaussian noise has been considered and it is necessary to compute the corresponding parameters for the generation of noise.

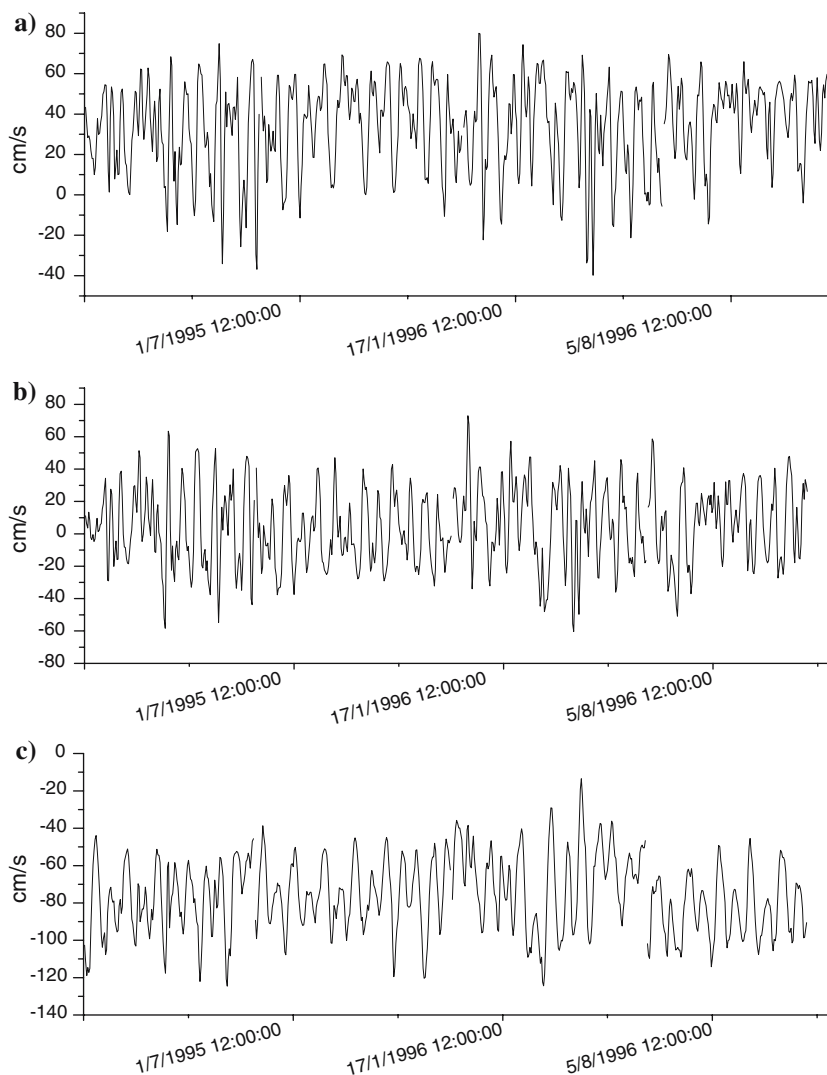
The parameters of the Gaussian noise were computed from the histograms for the u_{depth}^{24} series for all available depths. In Fig. 2, the daily mean flow at 75, 125 and 225 m depth are presented. The 75 m depth for the ‘pure’ Atlantic inflow layer, the 225 m depth for the ‘pure’ Mediterranean outflow layer and the 125 m depth is a typical depth for the interface at the main sill of the Gibraltar Strait on a long term scale. The time series are not harmonic and they are composed by the harmonic subinertial signals and noise. In Fig. 3, the relative histograms (the noisy line) of the three selected and representative depths are also shown. From the computation of the frequency histograms for the available depth it is easy to see that they have a bi-modal distribution except for the 225 m depth case.

Several two-modal analytical functions were contrived to fit the experimental distribution. A very common procedure from X-ray spectroscopy was used in order to solve the problem. Since the 1970s the *Rietveld Method* or *Rietveld Refinement* is widely used to fit X-ray spectra (Rietveld 1963). This allows us to fit of a linear combination of peak functions to an X-ray spectrum (Young 1995; Rietveld 1995; Toraya 1995). The more usual peak functions used in the Rietveld method are the Gaussian, the Lorentz and their linear combination in the pseudo-Voigt function (Young 1995). The pseudo-Voigt function is built by the weighted summation of a Lorentz and a Gaussian functions (*L*-contribution and *G*-contribution, respectively). Although it is usually formulated with the same location (Young 1995), it can be easily extended for two peaks with different one. The pseudo-Voigt function for two peaks with different locations in the *x*-axis, considering the values of the coefficients given by Young (1995) reads as:

$$pV(x) = (1 - \eta) \frac{4 \ln(2)}{D_G \sqrt{\pi}} \exp \left(-2.7726 \frac{(x - \bar{G})^2}{D_G^2} \right) + \eta \frac{2}{D_L \pi} \frac{1}{1 + 4 \frac{(x - \bar{L})^2}{D_L^2}}, \quad (2)$$

where the first term is the *G* contribution function and the second is the *L* contribution. For currents

Fig. 2 Time series of the daily mean flux at 75, 125 and 225 m depths



expressed in cm/s, η is a mixture dimensionless weighting parameter with $\eta \in [0, 1]$; \bar{L} and \bar{G} are the x -axis positions of the L -contribution and G -contribution in cm/s; D_L and D_G are their standard deviations in cm/s also. It is straightforward to verify that Eq. 2) verifies all the requirements of the probability function.

Each frequency histogram was fitted to the generalised pseudo-Voigt equation (Eq. 2) by the Levenberg–Marquardt method (Press et al. 1986) in order to obtain the best estimations of the five adjustable parameters in the sense of least squares. The fitting of the pseudo-Voigt function is highly non-linear because the analytical form of the L and G functions. The inclusion of the dimensionless weighting parameter increases the difficulty of the numerical procedure. However this problem is very efficiently solved by the use of a constrained Levenberg–Marquardt method by the assignment of an interval to the location of L -contribution and G -contribution from the analysis of

the frequency histograms. With this, the convergence of the fits was accelerated and the quality of the fit was drastically improved. In each of the cases the correlation coefficient was greater than 0.83. The parameters obtained from the non-linear fitting are presented in Table 3 and could be biased due to the unavoidable experimental errors. The superposition of experimental probability function and the corresponding pseudo-Voigt function are also shown for 75, 125 and 225 m depths in Fig. 3 (smoothed lines). Since the histograms were not previously smoothed for the fits and the correlation coefficients seem small, the non-linear fits have a high quality. The only exception with three peaks structure is at 225 m depth. Some additional fits were also tried considering additional Gaussian distributions but the results are quite un-sensitive to more complex structure at only one depth. A collateral result is the mean regime of the current at any depth that can be easily computed from the cumulative numerical

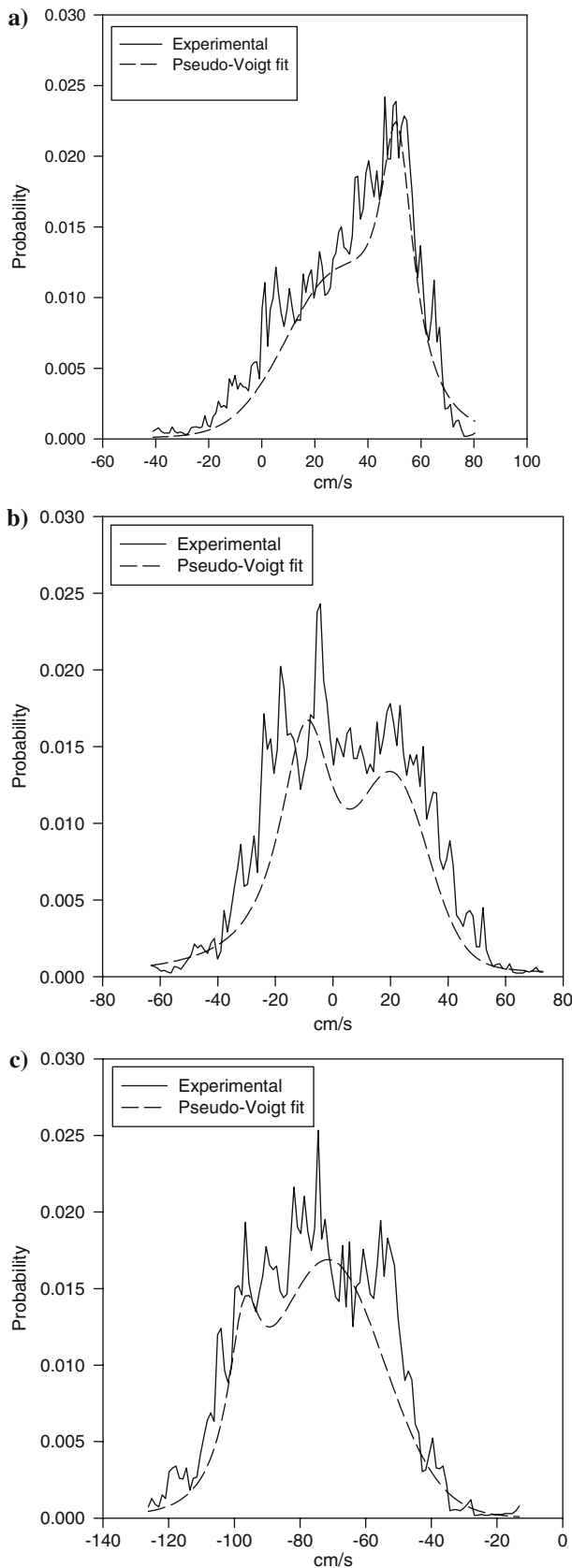


Fig. 3 **a** Relative frequency histogram and fit of the analytical function for the subinertial signal at 75 m depth. *Solid line* (noisy) corresponds to the frequency histogram and the *dashed one* (smooth) corresponds to the analytical function. **b** Same but for 125 m depth time series. **c** Same but for 225 m depth time series

integration of the Eq. 2 with the corresponding parameters in Table 3 as:

$$P(u_{\text{depth}}^{24} < u) = \int_{u_{\text{min}}}^u pV(x) \cdot dx \tag{3}$$

5.1 Preliminary discussion

In order to discuss the parameters of Table 3, their plots are presented in Fig. 4a–c. In Fig. 4a, the dimensionless weighting factor is plotted in depth. Here, η gives the proportion of each contribution, L or G , over depth. The area to the left of the curve belongs to the L -contribution and the area to the right corresponds to the G -contribution. Four segments can be distinguished. The first one from 45 to 115 m depth, the second one from 125 to 175 m depth, the third one from 185 to 225 m depth and the last from 225 m to the last available depth at 255 m. The first segment can be clearly associated with the Atlantic inflow layer. The second segment is associated with the interface layer and the two deepest with the Mediterranean outflow layer. The upper of the two is not affected by some undetermined phenomenon that increases the Gaussian contribution. In the Atlantic inflow layer the average weight factor is over 0.45, implying that the G -contribution is about 55% of the total variance. The second layer belongs to the usual depth of the interface location. The weight factor is greater than 0.20 with about 80% of G -contribution, denoting an extremely high variability of the mean flow at such depths. Below the interface layer it is possible to distinguish two sub-layers. The upper one can be assigned to the ‘pure’ Mediterranean outflow with a weight factor exceeding 0.60 and 40% of the G -contribution and the lower one with a weight factor of 0.15 or 85% of the G -contribution. The reason of why the mixture parameter obtains these values requires further studies and the use of fully nonlinear numerical model.

Notice that the standard deviation of all estimates increases when η decreases (Table 2), when the G -contribution is higher. This is general and affects all

Table 3 Parameters of the fitting of the pseudo-Voigt function

Depth(m)	\bar{G}	D_G	\bar{L}	D_L	η
45	35.29 (5.03)	40.48 (6.81)	53.27 (0.46)	15.31 (3.91)	0.42 (0.19)
55	32.14 (5.16)	42.33 (7.54)	52.63 (0.44)	14.95 (3.25)	0.45 (0.17)
65	29.10 (4.72)	43.32 (7.55)	51.75 (0.44)	15.33 (2.76)	0.46 (0.14)
75	27.34 (4.32)	44.34 (7.04)	51.00 (0.50)	14.85 (3.03)	0.41 (0.14)
85	23.85 (3.04)	45.18 (5.18)	49.03 (0.44)	13.45 (2.46)	0.36 (0.09)
95	17.28 (2.47)	43.35 (4.95)	45.04 (0.53)	14.30 (2.17)	0.37 (0.08)
105	8.34 (1.70)	38.52 (3.99)	39.01 (0.63)	15.21 (1.84)	0.42 (0.06)
115	0.07 (1.42)	35.20 (3.50)	31.89 (0.80)	16.52 (2.13)	0.42 (0.06)
125	21.48 (1.64)	27.66 (4.30)	-9.02 (1.36)	23.58 (2.96)	0.61 (0.07)
135	-1.52 (2.36)	42.06 (4.37)	-26.54 (0.63)	10.51 (3.06)	0.23 (0.09)
145	-14.64 (3.10)	35.85 (5.02)	-33.73 (0.73)	10.71 (4.18)	0.25 (0.14)
155	26.23 (3.56)	29.24 (5.26)	-40.13 (0.71)	11.28 (4.37)	0.30 (0.22)
165	-38.22 (2.05)	24.26 (3.22)	-50.69 (0.74)	8.26 (4.33)	0.19 (0.16)
175	-46.69 (1.08)	24.40 (2.80)	-59.82 (0.59)	6.99 (3.30)	0.18 (0.12)
185	-47.28 (1.04)	18.34 (2.54)	-64.58 (0.73)	13.04 (1.46)	0.56 (0.07)
195	-51.67 (1.35)	21.67 (3.16)	-70.89 (0.91)	16.16 (1.61)	0.58 (0.08)
205	-54.18 (1.04)	20.32 (2.72)	-75.88 (0.90)	19.26 (1.69)	0.64 (0.06)
215	-68.76 (1.73)	37.84 (3.41)	-92.56 (1.02)	10.57 (4.52)	0.14 (0.08)
225	-70.88 (1.81)	39.14 (3.79)	-96.96 (1.05)	11.84 (4.18)	0.18 (0.08)
235	-70.21 (2.22)	38.22 (4.63)	-96.24 (1.29)	15.93 (3.99)	0.27 (0.10)
245	-69.80 (2.04)	39.17 (4.29)	-96.59 (1.12)	15.17 (3.71)	0.26 (0.09)
255	-69.65 (1.30)	42.53 (2.85)	-99.34 (0.58)	7.45 (2.24)	0.14 (0.04)

First column is the depth in meters, the second and third are the position and standard deviation of G -contribution, respectively. Next two are the same but for L -contribution (all in cm/s) and the last one is the dimensionless weight or mixture factor. Between parenthesis the standard deviations of all estimates from fits

parameter estimates complicating the fits. They also present higher values at interface depths and close to the bottom compared to the other depths where the G -contribution is higher.

The depth distributions of G and L -contributions are shown in Fig. 4b. The shape of the vertical profile of the L -contribution (dotted line) is a quasi two layer flow with a constant upper part of 50 cm/s, a bottom layer part exceeding -96 cm/s and an intermediate transition layer with a zero crossing. The mean interface depth is located between 115 and 125 m depth where a sudden change in the mean flow occurs from 31.89 to -9.02 cm/s occurs. Hence, the depth of interface over 120 m is a good option for two-layer models over the sill. This vertical profile can be associated to the long-term steady two-layer dynamic in the Strait of Gibraltar. The G -contribution (solid line) shows a similar vertical profile with the same layers but with an abrupt change in the behaviour between 115 and 125 m, where the mean depth of the interface was found from the L -contribution analysis. This change implies a drastic modification in the trend of the vertical profile. The depth of the mean location of the interface coincides with the inversion of the L and G contribution locations and the Atlantic inflow layer is thinner than the Mediterranean one.

Finally, the weighted variances ($\eta D^2_{L,(1-\eta) D^2_G}$) of the two contributions are plotted in Fig. 4c.

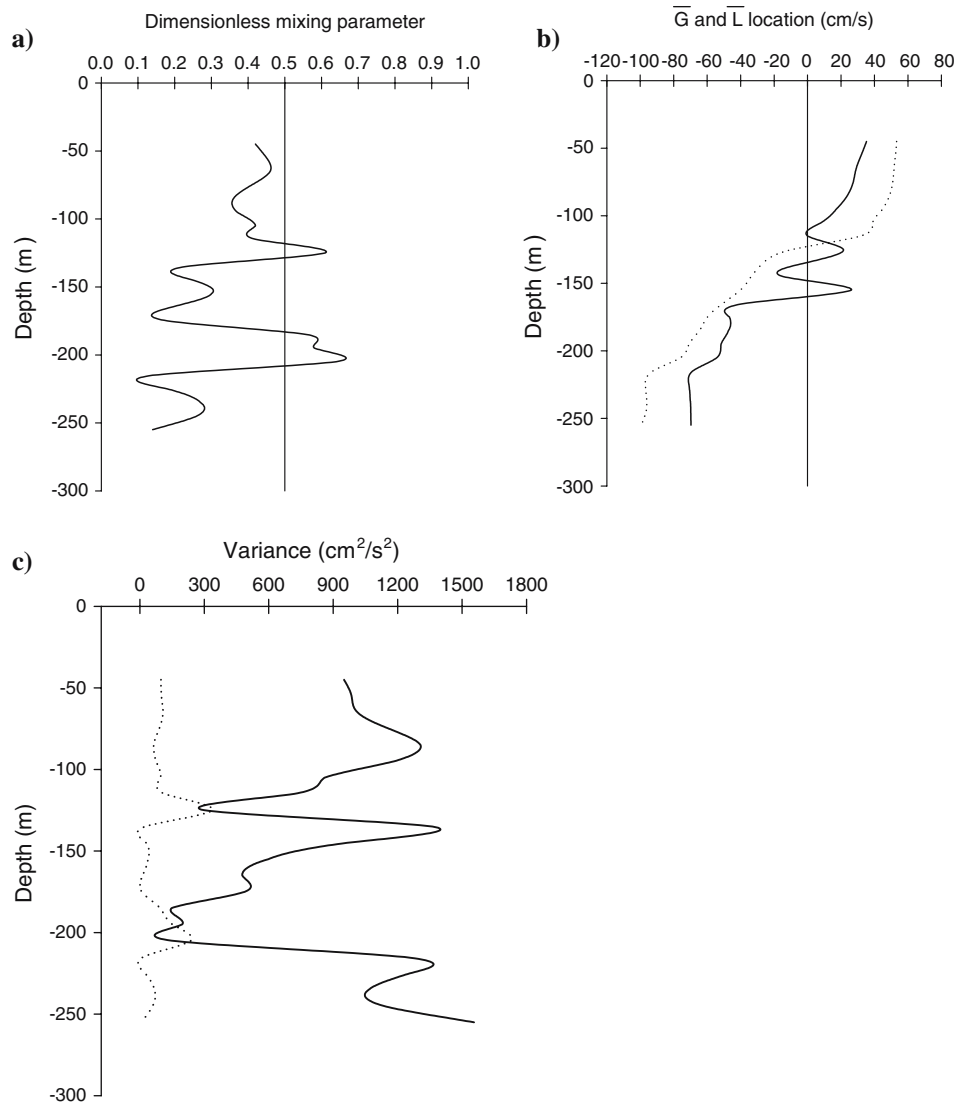
Because the G -contribution (solid line) is wider than the L -contribution (dotted line) the standard deviation of the second is always smaller. At these estimates, the G -contribution variance is always much greater than the L -contribution. Only at the depth of the interface and below 200 m they are approximately equal.

Taking into account that the vertical profile of the L -contribution is similar to the vertical distribution of the long term current in the Strait of Gibraltar, it is possible to hypothesize that the sub-inertial distortions of the currents are summarized in the G -contribution. Hence, in order to include it in the numerical experiments, a sequence of Gaussian random numbers $N(\bar{G}, (1-\eta)D_G^2)$ for each depth with the parameters of Table 3 will be generated. They will be used in the simulation of the next section.

6 Numerical experiments

Once the mathematical model is formulated for the ILW, the model is solved many times introducing the corresponding noise structures (see Sect. 5) at each of the depths. The resonant wavelengths are computed for each simulation and the frequency histogram of the obtained wavelengths is plotted.

Fig. 4 **a** Dimensionless weight factor vertical profile; **b** Location of G and L contributions over depth; **c** Variance of G and L contributions in depth. The *solid line* corresponds to the G contribution and the *dotted one* for the L contribution in Figs **b** and **c**



6.1 Computation of resonant wavelengths: the Taylor–Goldstein equation

The generation of ILWs in a continuously stratified flow can be investigated from the Taylor–Goldstein equation following Kundu (1990), Konyaev and Sabinin (1992), Bruno et al. (2002), Alonso et al. (2003) or with an extended high order model in Alonso and Andonegui (2005):

$$\hat{\psi}_{zz} + q(z)\hat{\psi} = k^2\hat{\psi}. \tag{4a}$$

This is obtained by taken the equations of motion (Kundu 1990; Bruno et al. 2002; Alonso et al. 2003; Nakamura et al. 2000) neglecting rotation, viscosity and the non-linear terms, introducing the stream function and taking normal modes. Here, $\hat{\psi}$ is the complex

amplitude of the stream function and the potential function is:

$$q(z) = \frac{N^2}{(U - c)^2} - \frac{U_{zz}}{(U - c)}, \tag{4b}$$

where $U(z)$ is the background horizontal velocity, $N^2(z)$ is the buoyancy frequency and c is the phase speed of the internal wave. Subscripts indicate derivatives. Eq. 4a together with the boundary conditions $\hat{\psi}(0) = \hat{\psi}(h) = 0$, is a harmonic Sturm–Liouville problem where the solutions are the eigenvectors, $\hat{\psi}_n$, with their corresponding eigenvalues, k_n^2 . The eigenvectors satisfy the orthogonality condition as usual.

The Sturm–Liouville problem for an arbitrary potential function must be solved numerically. There are several numerical standard methods to do it,

among which are those related in Henrici (1962) and Bailey et al. (1991). The latter, based in the Prüfer decomposition instead the eigen-decomposition of the coefficient matrix, severely affected by round off errors in the former, is the best one but useful for the smallest eigenvector. The interest is in the internal waves that can be resonant, in other words in the internal waves with zero velocity relative to the flow phase velocity of the flow, $c = 0$ (Bogucki et al. 1999; Bruno et al. 2002; Alonso et al. 2003; Alonso and Andonegui 2005). Since the solution of Eq. 4a is not unique, the *topographic criterion for its existence* was applied (Alonso et al. 2003). In the same paper it was demonstrated numerically that at least one of the wavelengths determined from the bottom topography could be found in the ILW wavelength spectrum.

The vertical profile of the background velocity is computed from harmonic prediction without considering the subinertial frequency band. The buoyancy frequency is easily computed from Eq. 1.

6.2 Numerical experiments and discussion

Although it is possible to perform the following analysis at any moment of the tidal cycle because the harmonic prediction of the velocity field, five time moments of ILW generation were considered. The vertical profile of the background velocity is computed from the harmonic constants of the current at all available depths (Alonso et al. 2003). After that, a random number $N(\overline{G}(z), (1 - \eta(z))D_G^2(z))$ is generated and added to the corresponding depth from the corresponding parameters of Table 3. The Sturm–Liouville problem is solved using the background velocity perturbed by the subinertial noise. The resonant wavelengths for the unperturbed problem and the corresponding times in GMT are given in Table 4. Each one of the five simulations has 15,000 profiles of noise. The profiles of the potential function are shown in Fig. 5.

The normalized histograms of the wavelength of each case are presented in Fig. 6. The solutions of the noise free problems coincide with the maximum of the frequency distribution except for case e (Fig. 6e). A continuous spreading of wavelengths around the wavelength of the noise free solution can be observed. In cases a, b, and e (Fig. 6a, b, e), a high probability of ILW inhibition is observed (zero wavelength). This means that the subinertial noise is capable of inhibiting the generation of ILW. In case e (Fig. 6e) the inhibition is almost complete. The explanation of this last result lies in the field of the physics of the ILW phenomenon. The ILW occurs with a suitable combination of stratification and background velocity. If

Table 4 Analysed time moments and resonant wavelengths for the unperturbed problems

Case number	Hours (GMT)	Date	Unperturbed wavelength (m)
A	16 00	11/24/98	1151
B	16 00	11/25/98	1220
C	15 00	11/27/98	1884
D	20 00	11/29/98	1029
E	22 00	11/29/98	1484

their combination is not stable in the presence of a perturbation (i.e. a subinertial noise) then the generation of the ILWs is inhibited. From the knowledge of the authors, there is no criterion to predict the ILW inhibition. That kind of highly theoretical work must be left for further works.

7 Stability analysis

Hazel (1972) developed an elegant and clear mathematical analysis of stability for many standard cases based in the Taylor–Goldstein equation. We shall follow his ideas with some modifications. His analysis consisted of the joint representation of dimensionless wavelength and the dimensionless Richardson number. However the procedure for getting the dimensionless expression of the Taylor–Goldstein equation is quite unphysical. The curves in such a phase space are named single neutral modes (SNM) and respond to a curve $J_0 = \alpha(1-\alpha)$ as a function of the dimensionless wavenumber, $\alpha = kh$, where k is the wavenumber and h is a certain reference depth. This fixes the SNM of maximum stability. In this study such an approach cannot be applied because the cases correspond to a

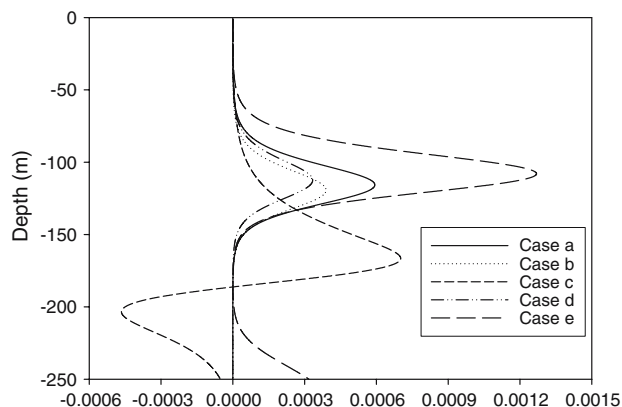
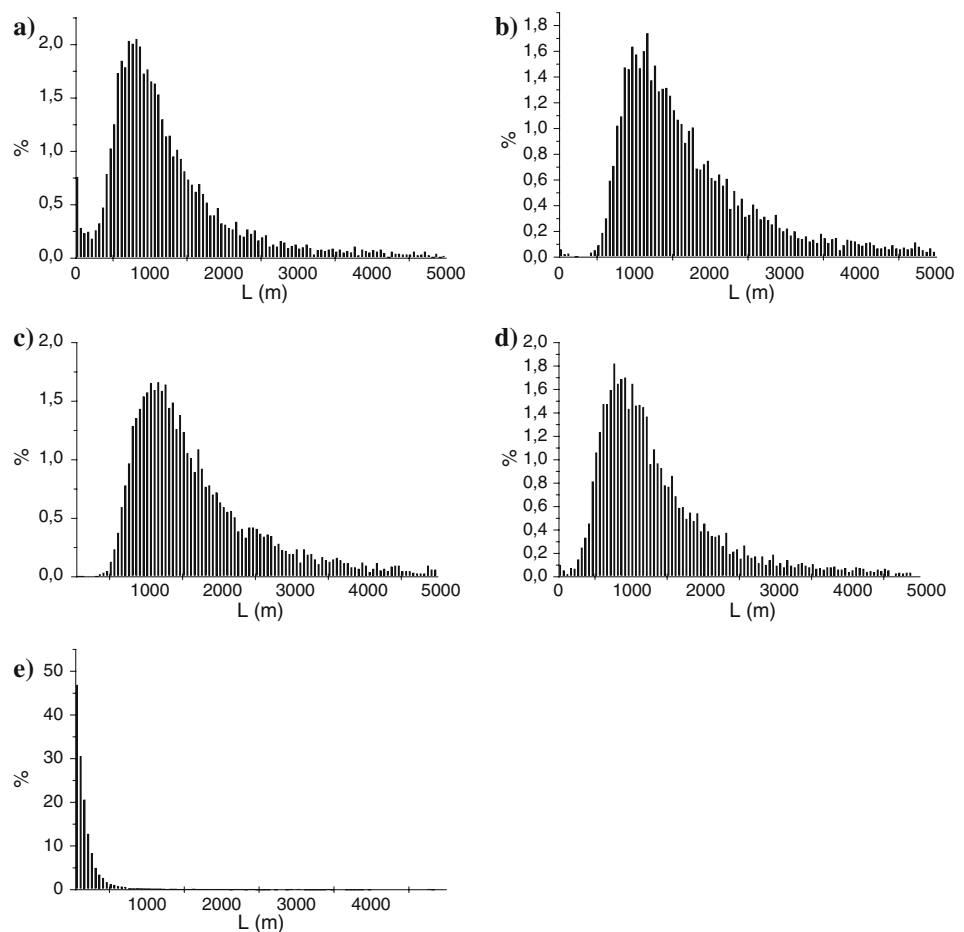


Fig. 5 Vertical profiles of the potential function for the cases of Table 4

Fig. 6 Frequency histograms for the resonant wavelengths for the cases given in Table 4



single point in the Hazel’s diagrams, in particular when the stability of the water column follows a hyperbolic tangent profile. The critical depth or limit given by Hazel (1972) is $z/h \in [1.195, 1.25]$. The theoretical interval of Hazel is accomplished if the depth of the interface is 50 m. Obviously this happens in the Strait of Gibraltar at a few moments when the interface is close to the surface. From the observations, the depth of the interface is about 125 m depth and the number of reference is 2.5 (depth of the sill/depth of the interface), this must be considered the critical limit for this work and it will be a more complex function depending on the $q(z)$ (Eq. 4b).

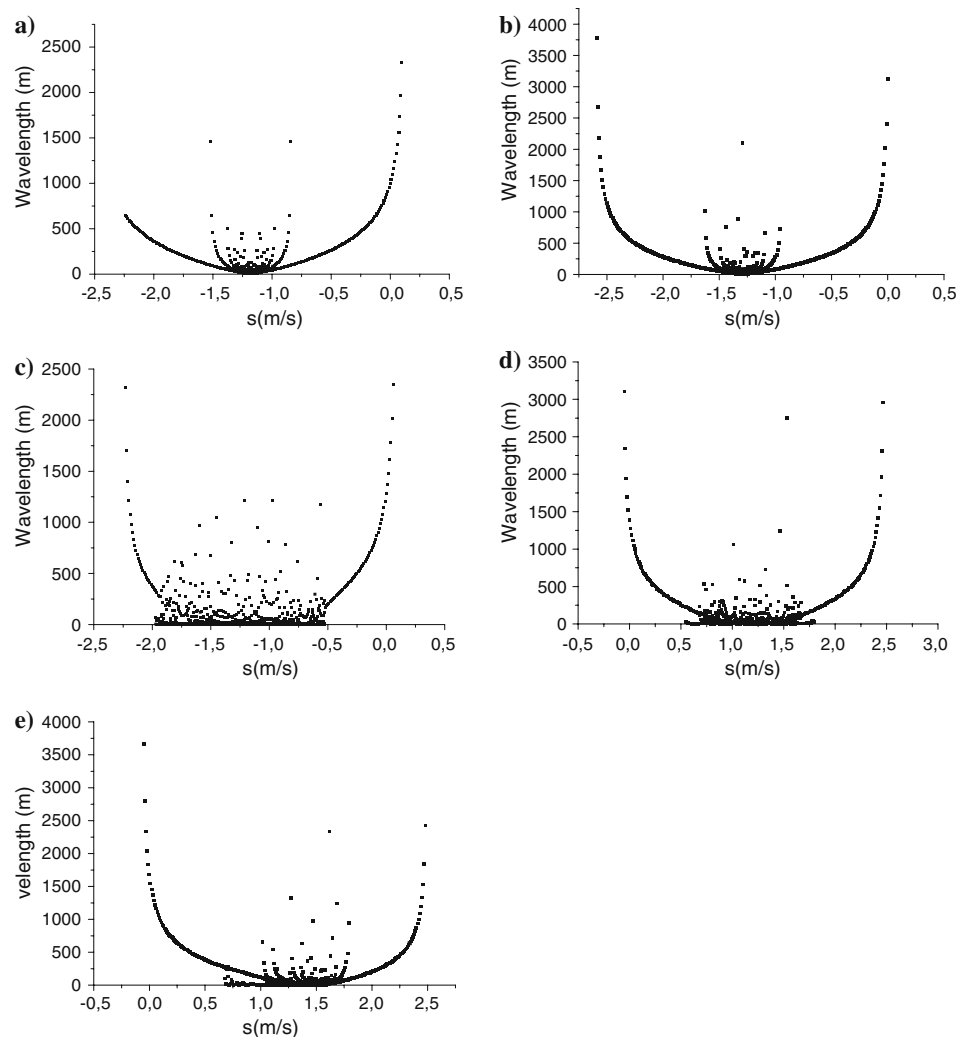
In order to build a dispersion relationship plot for the selected cases, the Taylor–Goldstein equation (Eq. 4a) can be treated as the dispersion relationship if different values of a barotropic subinertial current (named s) are added to $U(z)$. For the five cases the unrealistic, but useful to fix ideas, interval $[-3,3]$ m/s was finely scanned ($\Delta s = 0.01$ m/s) in order to obtain good representations of the subinertial dispersion relationships. Positive values of s denoted subinertial currents towards the Atlantic and negative towards the Mediterranean. Results are presented in Fig. 7,

corresponding to the analysed cases of Table 4. The value of the computed wavelength when $s = 0$ is the same as presented in Table 4. In all cases the result for $s = 0$ corresponds to situations far away from the central and most complicated zone.

Smooth branches forming parabola can be distinguished in all plots. They are the SNMs of the Hazel’s analysis and represent the evolution of the wavelength of the most stable oscillation mode when changing the velocity of the wave. Several solutions can appear for a determined value of s , given principal and secondary modes. In general, the secondary branches are not symmetrical around the minimum value of the wavelength defined by the main ones. There are many combinations of $\{s, L\}$ where the ILWs are not generated. They correspond to the places out of limits of the wider parabola and between the branches.

Cases a and b are the most stable because the spreading is lesser than in cases c, d and e (Fig. 5). This is related to the shape of the dispersion relationships. For cases a and b, the branches are well defined and few solutions are allowed. For cases c, d and e, many solutions can appear and the curves in the middle present many branches. Cases c, d and e have a branch

Fig. 7 Dispersion relationship relative to subinertial barotropic current for the cases of Table 4



running on the zero wavelength line. In addition, in cases d and e the $s = 0$ solution is to the left and in the other cases to the right of the central position of zero wavelength.

8 Conclusions

Simulations of the influence of noise on the generation of ILW were carried out. In order to perform the simulation it was necessary to establish the characteristics of the noise in the water column. Hence the Gaussian subinertial noise was parameterized at all the depths and simulations were carried out in five selected cases: two correspond to very stable conditions, two are related to medium stability conditions and one is fully unstable. The results lead to a continuous spreading of the distribution of wavelengths, implying that the presence of noise greatly distorts the generation of ILW and it is capable of inhibiting them.

A stability analysis is also carried out following and extending the ideas of Hazel (1972). The dispersion relationships obtained present many branches corresponding to a SNM and fixing the combinations (s , L) without generating ILW. If the unperturbed solution ($s = 0$) lies to the left of the central point of the dispersion relationships plot the distribution of the wavelengths represents higher spreading. In addition small increments in the subinertial barotropic current affect strongly the wavelength of the ILW.

This kind of analysis has the advantages that covers most of the cases of ILW generation and leads to the possibility of obtaining the probabilities of occurrence of the phenomenon. This leads to the possibility of improving the design and timing of oceanographic surveys devoted to the study of ILW in any strait.

Acknowledgments J. Alonso is grateful to Dr R. L. Haney for the very interesting discussion and ideas when visited the Naval Postgraduate School (Monterey, California) supported with the

ONR-VSP-4036 grant. Authors are also grateful to Dr M. Piñero from the Applied Physics Department of the University of Cádiz for his help in the Rietveld's refinement and to the two anonymous referees that made interesting suggestions that improved the work. This work has been supported by the CGL2004-01473/CLI CICYT project of the Spanish Government and the RNM337 of the Andalusia Government.

References

- Alonso JJ, Andonegui E (2005) A linear high order formulation for internal lee waves in the Strait of Gibraltar. *J Mar Syst* 53:197–216
- Alonso JJ, Bruno M, Vázquez A (2003) On the influence of tidal hydrodynamic conditions in the generation of internal resonant waves at the main sill of the Strait of Gibraltar. *Deep Sea Res I* 50:1005–1021
- Bailey PB, Garbow BS, Kaper HG, Zetti A (1991) Transactions on Mathematical Software, vol 17 N 4 December, 1991, pp 500–501
- Baines PG (1982) On internal tide generation models. *Deep Sea Res* 29:307–338
- Bogucki D, Redekopp LG, Dickey T (1999) Sediment resuspension and mixing by resonantly generated internal solitary waves. *J Phys Oceanogr* 27:1181–1196
- Brandt P, Alpers W, Backhaus JO (1996) Study of the generation and propagation of the internal waves in the Strait of Gibraltar using a numerical model and synthetic aperture radar images of the European ERS—a satellite. *J Geophys Res* 101:14327–14252
- Bray NA, Winant CD, Kinder TH, Candela J (1990) Generation and kinematics of the internal tide in the Strait of Gibraltar. In: Pratt L (ed) *The physical oceanography of sea straits*. Kluwer, Dordrecht
- Bruno M, Mañanes R, Alonso J, Tejedor L, Kagan B (2000) Vertical structure of the semidiurnal tidal currents at Camarinal Sill, the Strait of Gibraltar. *Oceanol Acta* 23(1):15–24
- Bruno M, Alonso J, Cózar A, Vidal J, Echevarría F, Ruiz J, Ruiz A (2002) The boiling water phenomena at Camarinal Sill, the Strait of Gibraltar. *Deep Sea Res II* 49:4097–4113
- Candela J, Winant CD, Bryden HL (1989) Meteorologically forced subinertial flows through the Strait of Gibraltar. *J Geophys Res* 94:12667–12674
- Candela J, Winant CD, Ruíz A (1990) Tides in the Strait of Gibraltar. *J Geophys Res* 95:7317–7335
- CANIGO (1999) Final scientific report. MAST III, CT96-0060
- Cavanie AG (1972) Observations de fronts internes dans le détroit de Gibraltar pendant la Campagne Océanographique OTAN 1970 et interpretation des résultats par un modèle mathématique. *Mémoires de la Société des Sciences de Liège* 6:27–41
- Crépon M (1965) Influence de la pression atmosphérique sur le niveau moyen de la Méditerranée Occidentale et sur le flux à travers le Détroit de Gibraltar. *Cah Oceanogr* 1:12–32
- Echevarría F, Gómez F, García Lafuente J, Gorsky G, Goutx M, González N, Bruno M, García C, Vargas JM, Picheral M, Striby L, Alonso del Rosario J, Reul A, Cózar A, Prieto L, Jiménez-Gómez F, Varela M (2002) Physical–biological coupling in the Strait of Gibraltar. *Deep Sea Res II* 49:4115–4130
- Frassetto R (1964) Short period vertical displacements of the upper layers in the Strait of Gibraltar. *Tech. Rep. 30, SACLANT ASW, Res. Center, La Spezia, Italy*
- Freeland HJ, Farmer DM (1980) Circulation and energetics of a deep strongly-stratified inlet. *Can J Fish Aquat Sci* 37(9):1398–1410
- Garrett CJR, Munk WH (1972) Space–Time scales of internal waves. *Geophys Fluid Dyn* 3:225–264
- Garrett C, Akerly J, Thompson K (1989) Low frequency fluctuations in the Strait of Gibraltar from MEDALPEX sea level data. *J Phys Oceanogr* 19:1682–1696
- Gerkema T, Zimmerman JTF (1995) Generation of nonlinear internal tide and solitary waves. *J Phys Oceanogr* 25:1081–1094
- Geyer WR, Cannon GA (1982) Sill processes related to deep water renewal in a fjord. *J Geophys Res* 87:7985–7996
- Gill AE (1982) Atmosphere–ocean dynamics. In: William L. Donn (ed) *International geophysics series*. Academic, New York
- Griffin DA, LeBlond PH (1990) Estuary–Ocean exchange controlled by spring-neap tidal mixing. *Est Coast Shelf Sci* 30:275–297
- Hazel P (1972) Numerical studies of the stability of inviscid stratified shear flow. *J Fluid Mech* 51(1):39–62
- Henrici P (1962) *Discrete variable methods in ordinary differential equations*, Wiley, New York
- Hibiya T (1986) Generation mechanism of internal waves by tidal flow over a sill. *J Geophys Res* 91:7696–7708
- Hibiya T, Ogasawara M, Niwa Y (1998) A numerical study of the fortnightly modulation of basin–ocean water exchange across a tidal mixing zone. *J Phys Oceanogr* 28:1224–1235
- Huthnance JM (1989) Internal tides and waves near the continental shelf edge. *Geophys Astrophys Fluid Dyn* 48:81–106
- Konyaev KV, Sabinin KD (1992) *Waves inside the Ocean*. Gidrometeoizdat (in Russian)
- Kundu PJ (1990) *Fluids mechanics*. Academic, New York
- Lacombe H, Richez C (1982) The regimen of Strait of Gibraltar. In: De Nihoul J (ed) *Hydrodynamics of semi-enclosed seas*. Elsevier, New York, pp 13–73
- Lacombe H, Richez C (1984) *Hydrography and currents in the Strait of Gibraltar*. Office of Naval Research, Sea Straits Report 3, NORDA
- La Violette PE, Lacombe H (1988) Tidal induced pulses in the flow through the Strait of Gibraltar. *Oceanol Acta* SP 13–17
- La Violette PE, Kinder TH, Green DW (1986) Measurement of internal wave in the Strait of Gibraltar using shore based radar, technical report 118, Naval Ocean Research and Development Activity, National Space Technology Laboratory, Bay of St. Louis, p 13
- Lott F, Teitelbaum H (1993a) Topographic waves generated by a transient wind. *J Atmos Sci* 50:2607–2624
- Lott F, Teitelbaum H (1993b) Linear unsteady mountain waves. *Tellus* 45A:201–220
- Mañanes R, Bruno M, Alonso J, Fraguera B, Tejedor L (1998) Non-linear interaction between tidal and subinertial barotropic flows in the Strait of Gibraltar. *Oceanol Acta* 21(1):33–46
- Morozov EG, Trulsen K, Velarde MG, Vlasenko VI (2002) Internal tides in the Strait of Gibraltar. *J Phys Oceanogr* 32:3193–3206
- Nakamura T, Awaji T (2001) A growth mechanism for topographic internal waves generated by an oscillatory flow. *J Phys Oceanogr* V31:2511–2524
- Nakamura T, Awaji T, Hatayama T, Akitomo K, Takizawa T, Kono T, Kawasaki Y, Fukasawa M (2000) The generation of large-amplitude unsteady Lee Waves by Subinertial K1 tidal flow: a possible vertical mixing mechanism in the Kuril Strait. *J Phys Oceanogr* V30:1601–1621

- Nunes RA, Lennon GW (1987) Episodic stratification and gravity currents in marine environment of modulated turbulence. *J Geophys Res* 92(C5):5465–5480
- Pillsbury R, Barstow D, Botero J, Millero C, More B, Pittock G, Root D, Simpkins J, Still R, Bryden H (1987) Gibraltar experiment: current measurements in the Strait of Gibraltar. Oregon State University Technical report 87:29–284, pp 477–491
- Press WH, Flannery BP, Teukolsky SA, Vetterling WT (1986) Numerical recipes, Cambridge University Press, Cambridge
- Richez C (1994) Airborne synthetic aperture radar tracking of internal waves in the Strait of Gibraltar. *Prog Oceanogr* 33:93–159
- Rietveld HM (1995) The early days: a retrospective view. In: Young RA (ed) *The Rietveld method*. International union of crystallography, Oxford University Press, Oxford, pp 39–42
- de Silva Samarasinghe JR, Lennon GW (1987) Hypersalinity, flushing and transient salt-wedges in a Tidal Gulf—an inverse estuary. *Estuar Coastal Shelf Sci* 24:483–498
- Toraya H (1995) Position-constrained and unconstrained powder-pattern-decomposition methods. In: Young RA (ed) *The Rietveld method*, international union of crystallography, Oxford University Press, pp 254–275
- Tsimplis MN (2000) Vertical structure of tidal currents over the Camarinal sill at the Strait of Gibraltar. *J Geophys Res* 15:19709–19728
- Tsimplis M, Bryden H (2000) Estimation of the transports through the Strait of Gibraltar. *Deep Sea Res I* 47:2219–2242
- Valle-Levinson A, Wilson RE (1994) Effects of barotropic forcing and vertical mixing on estuary/ocean exchange. *J Geophys Res* 99:5149–5169
- Watson G, Robinson LS (1990) A study on internal wave propagation in the Strait of Gibraltar using shore-based radar images. *J Phys Oceanogr* 20:374–395
- Wunsch C (1969) Progressive internal waves on slopes. *J Fluid Mech* 35:131–144
- Young RA (1995) Introduction to the Rietveld method. In: Young RA (ed) *The Rietveld method*, international union of crystallography, Oxford University Press, pp 1–38
- Ziegenbein J (1969) Short internal waves in the Strait of Gibraltar. *Deep Sea Res* 16:479–487